Regular Article

Anisotropic tight-binding model applied to zigzag ultra-small nanotubes

A.N. Ribeiro^a and C.A. Macedo

Departamento de Fisica, Universidade Federal de Sergipe, 49100-000 Sao Cristovao-SE, Brazil

Received 9 September 2009 / Received in final form 21 January 2010 Published online 24 March 2010 – © EDP Sciences, Società Italiana di Fisica, Springer-Verlag 2010

Abstract. A single-wall carbon nanotube (SWCNT) can be visualized as a graphene rolled into a cylinder. Tight-binding band structure calculations, with hopping between nearest-neighbor π orbitals only (NNTB), established rules by which both the mode in which the graphene is rolled up and the diameter determine whether the SWCNT is a metal or a semiconductor. However, when the diameter of the SWCNT is ultra-small its large curvature results in the breakage of these rules. In this work, we studied zigzag (n, 0) SWCNTs with diameters smaller than 0.7 nm using a π orbital-only tight-binding model including anisotropy in the hopping between next-nearest-neighbor sites (ANNNTB). Band overlaps were found in the electronic band structures of the zigzag SWCNTs for n=3,4,5, and 6, indicating that they are metals. The reason why the band structures of armchair and chiral SWCNTs are less affected by curvature effects becomes clear with the ANNNTB model, as does the reason why non-degenerate states cause band overlaps of the zigzag SWCNTs for n=3,4,5, and 6. Our results show that a π orbital-only tight-binding model is able to describe both the band overlaps and gaps obtained by ab initio calculations for zigzag SWCNTs.

1 Introduction

Since the discovery of carbon nanotubes (CNT) by Iijima in 1991 [1], much effort has been employed towards the production of CNTs with ultra-small diameters. In 1992, Ajayan and Ijima reported the obtainment of a CNT with a diameter of 0.7 nm [2]. This remained the record for eight years, until Sun et al. reported the creation of a CNT with a diameter of 0.5 nm [3]. In that same year, fabrications of CNTs with diameters of 0.4 nm and 0.33 nm were reported [4–6]. In 2004, a CNT with an incredible diameter of 0.28 nm was reported by Zhao et al. [7], who considered the diameter to be the distance between two dark lines associated with nanotube walls in conventional highresolution transmission electron microscopy (HR-TEM) images. Recently, Guan et al. contested the reliability of the values of the calculated diameters and reported the smallest CNT as being 0.4 nm in diameter [8]. This measure was calculated using a modern HR-TEM with a post-specimen aberration corrector.

Single-wall carbon nanotubes (SWCNT) can be visualized as a graphite sheet (graphene) rolled into a cylinder. The SWCNTs are characterized by two integer numbers (n, m) that determine the modes as the graphene is rolled up. Zigzag SWCNTs are characterized by indices (n, 0). Tight-binding band structure calculations with hopping

between nearest-neighbor π orbitals only (NNTB) showed that both the mode in which the graphene is rolled up and the diameter (d) determine the type of conductor a SWCNT is [9]. If 2n+m=3p (p) is an integer number then the SWCNT is a metal, otherwise it is a semiconductor [10,11]. This is the so called 1/3 rule. Further, the band gaps of SWCNT semiconductors are proportional to the inverse of their diameters [12], the so-called 1/d rule. However, when the diameter of the SWCNT is ultra-small, its large curvature results in the breakage of these rules.

Calculations using density-functional theory (DFT) with different approximations showed that the band gap of the semiconductor (7,0) zigzag SWCNT is strongly reduced in relation to that obtained by NNTB, making its band gap smaller than that of the (8,0) SWCNT. This consequently breaks the 1/d rule [13–15]. The calculations also determined that (4,0) and (5,0) zigzag SWCNTs are metals, which violates the 1/3 rule [14–24]. Nevertheless, it was found that the electronic band structures of armchair and chiral SWCNTs are less affected by large curvatures than those of zigzag SWCNTs [18,19,21,25]; however, the reason for this is still an open question.

Blase et al. attribute these discrepancies between the ab initio and NNTB results to the strong hybridization induced by the large curvature of these SWCNTs. The antibonding π^* and σ^* states mix and repel each other, resulting in a lowering of energy of (originally) purely π^* states [13]. They also reported that the band responsible

a e-mail: anevesr@gmail.com

for band overlap of the (6, 0) SWCNT, and for the reduction of the band gaps of the (7, 0) and (8, 0) SWCNTs, is non-degenerate, but they do not explain why.

Tight-binding electronic band structure calculations with curvature effects included were realized. Hamada, Sawada and Oshiyama used the 2s and 2p orbitals of a carbon atom as the basis set for expressing the tight-binding model (HSO model) [11], i.e., they considered π and σ orbitals. Nevertheless, they found a narrow-gap in the (6, 0) SWCNT, which is not in agreement with the DFT results that indicates that this nanotube is a metal [13– 15,19–21]. Recently, Miyake and Saito [20], using the HSO model, calculated the band gaps of zigzag SWCNTs with d < 1.5 nm and showed that the band gaps of semiconductor zigzag SWCNTs with diameters greater than that of the (6, 0) SWCNT agree with the 1/d rule; however, when the band gaps of semiconductor zigzag SWCNTs are calculated with DFT using local-density approximation (LDA) this agreement only occurs for the SWCNTs with diameters greater than that of the (8, 0) SWCNT. Beyond this, Miyake and Saito calculated the band gap for the (5, 0) SWCNT as being ~ 0.06 eV using the HSO model, and with LDA they found a band overlap of 1.2 eV [20].

Blase et al. made tight-binding calculations with hopping between nearest-neighbor and next-nearest-neighbor π orbitals for zigzag SWCNTs with $n=6,\,7,\,8,\,$ and 9 [13]. They found band gaps close to those obtained by Hamada et al. [11] except for that of the $(6,\,0)$ SWCNT, which presented a band gap of 0.05 eV, whereas Hamada et al. obtained a band gap of $\sim\!0.2$ eV. Yorikawa and Muramatsu theoretically studied the curvature effect on the band gaps of semiconductor SWCNTs using a tight-binding model that takes into account a mixing effect between π and σ orbitals [26]. They obtained an approximate expression of the band gap for SWCNTs. They found that the band gap of the $(8,\,0)$ SWCNT is larger than that of the $(7,\,0)$ SWCNT, which agrees with results obtained by Blase et al.

These results suggested the hypothesis that the π orbital alone is not sufficient to describe the electronic band structures of SWCNTs with ultra-small diameters. However, we show in this work that a π orbital in a tight-binding model is able to obtain the values for the band gaps and overlaps yielded by ab initio calculations of zigzag SWCNTs with ultra-small diameters if we consider these effects as being a consequence of an increase in the electronic transfer among next-nearest-neighbor π orbitals to the length of the circumferential direction. This model allows for a natural explanation of why the band structures of armchair and chiral nanotubes with ultra-small diameters are less affected by large curvatures. It can also explain why non-degenerate bands are so important for zigzag SWCNTs with ultra-small diameters.

The remainder of this paper is organized as follows: in Section 2 we introduce the π orbital in the tight-binding model used to describe the band structures of SWCNTs with ultra-small diameters; in Section 3, we present the results and discuss them; Section 4 is dedicated to our conclusions.

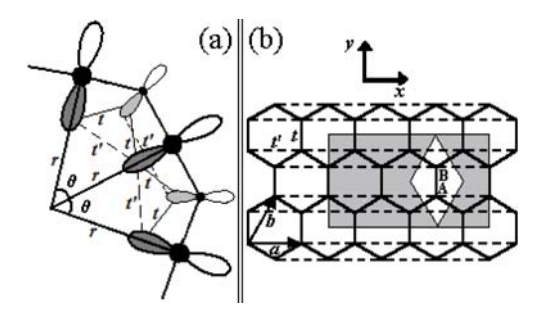


Fig. 1. (a) Schematic representation of the origin of the anisotropy due to the large curvature of the tube of a zigzag SWCNT with an ultra-small diameter. The electronic transfer energy between nearest-neighbor and next-nearest-neighbor sites are t and t', respectively. (b) Honeycomb lattice with anisotropic next-nearest-neighbor hopping. A unit cell of the (3,0) SWCNT is in gray and a unit cell of the two-dimensional lattice is inside the gray rectangle in white.

2 Anisotropic tight-binding model

In graphene, the π orbitals are perpendicular to the plane formed by carbon atoms and parallel to one another. Thus, when graphene is rolled up to form a nanotube, the π orbitals point out along the longitudinal axis of the nanotube. Therefore, the distance between the π orbitals along the circumferential direction is decreased. We consider that in zigzag nanotubes with ultra-small diameters the large curvature allows for a significant increase in the electronic transfer between the next-nearest-neighbor π orbitals located along the circumferential direction (see Fig. 1a). Thus, the simpler π orbital in a tight-binding model that describes zigzag SWCNTs with ultra-small diameters must consider, beyond the hopping between nearest-neighbor sites (t), the hopping between the two next-nearest-neighbor sites located along direction a with the same y coordinate (t') (see Fig. 1b), i.e., it must include anisotropic hopping between next-nearest-neighbor sites. The π orbitals are considered here to be perpendicular to the nanotube surface. In armchair and chiral nanotubes the next-nearest-neighbor π orbitals overlap less than on zigzag nanotubes because of the different rollup vectors of these nanotubes; hence, the increase in the electronic transfer between these orbitals in armchair and chiral nanotubes is smaller than in zigzag nanotubes. This explains why the band structures of armchair and chiral nanotubes are less affected by the curvature than the band structures of zigzag nanotubes.

The tight-binding energy dispersion relation of a zigzag SWCNT $[E_{(n,0)}]$ is obtained from the dispersion relation of the honeycomb lattice with the periodic boundary condition $n\mathbf{a} \cdot \mathbf{k} = 2\pi q \ (q = 1, 2, ..., 2n)$ in the circumferential direction and $L(-\mathbf{a} + 2\mathbf{b}) \cdot \mathbf{k} = 2\pi m$ (m = -L/2, -L/2 + 1, ..., L/2 - 1) in the longitudinal direction of the zigzag SWCNT, where $\mathbf{a} = a\mathbf{x}$ and $\mathbf{b} = (1/2)a\mathbf{x} + (3^{1/2}/2)a\mathbf{y}$ are honeycomb lattice unit vectors (see Fig. 1b) and L is the number of unit cells of the SWCNT [9]. The dispersion relation $[E(\mathbf{k})]$, in the Slater-Koster scheme, of the honeycomb lattice including

hopping between next-nearest neighbours in the direction a (as described in Fig. 1b) is given by the secular equation

$$\begin{vmatrix} H_{AA}(\mathbf{k}) - E(\mathbf{k}) & H_{AB}(\mathbf{k}) \\ H_{BA}(\mathbf{k}) & H_{BB}(\mathbf{k}) - E(\mathbf{k}) \end{vmatrix} = 0, \quad (1)$$

where

$$H_{AA} = \frac{1}{L} \sum_{\mathbf{R}_A} \sum_{\mathbf{R}'_A = \mathbf{R}_A} e^{-i\mathbf{k}(\mathbf{R}_A - \mathbf{R}'_A)}$$

$$\times \langle \varphi_A(\mathbf{r} - \mathbf{R}_A) | H | \varphi_A(\mathbf{r} - \mathbf{R}'_A) \rangle$$

$$+ \frac{1}{L} \sum_{\mathbf{R}_A} \sum_{\mathbf{R}'_A = \mathbf{R}_A \pm \mathbf{a}} e^{-i\mathbf{k}(\mathbf{R}_A - \mathbf{R}'_A)}$$

$$\times \langle \varphi_A(\mathbf{r} - \mathbf{R}_A) | H | \varphi_A(\mathbf{r} - \mathbf{R}'_A) \rangle$$

$$= \varepsilon_{2n} + 2t' \cos k_x a \qquad (2)$$

and

$$H_{AB} = \frac{1}{L} \sum_{\mathbf{R}_A} \sum_{\mathbf{R}_B = \mathbf{R}_A + a/\sqrt{3}y} e^{-i\mathbf{k}(\mathbf{R}_A - \mathbf{R}_B)}$$

$$\times \langle \varphi_A(\mathbf{r} - \mathbf{R}_A) | H | \varphi_B(\mathbf{r} - \mathbf{R}_B) \rangle$$

$$+ \frac{1}{L} \sum_{\mathbf{R}_A} \sum_{\mathbf{R}_B = \mathbf{R}_A \pm a/2x - a/(2\sqrt{3})y} e^{-i\mathbf{k}(\mathbf{R}_A - \mathbf{R}_B)}$$

$$\times \langle \varphi_A(\mathbf{r} - \mathbf{R}_A) | H | \varphi_B(\mathbf{r} - \mathbf{R}_B) \rangle.$$

$$= t \left(e^{-ik_y a/\sqrt{3}} + 2\cos(k_x a/2) e^{-ik_y a/(2\sqrt{3})} \right). \quad (3)$$

By using the equivalence of the A and B carbon atoms one has $H_{BB} = H_{AA}$; and H_{BA} is obtained by means of the Hermitian conjugation relation $H_{BA} = H_{AB}^*$. In this approximation the other terms with $|\mathbf{R}_A - \mathbf{R'}_A| = a$ and terms with $|\mathbf{R}_A - \mathbf{R'}_A| \ge 2a$ in equation (2), and terms with $|\mathbf{R}_A - \mathbf{R}_B| > a/3^{1/2}$ in equation (3) are neglected $(\mathbf{R}_A \text{ and } \mathbf{R'}_A \text{ are the position vectors of atoms } A \text{ and } \mathbf{R}_B$ is the position vector of atom B (Fig. 1b)). The orbital energy of the 2p level, ε_{2p} , and the transfer integrals, t and t', are given by

$$\varepsilon_{2p} = \langle \varphi_A(\mathbf{r} - \mathbf{R}_A) | H | \varphi_A(\mathbf{r} - \mathbf{R}_A) \rangle,$$
 (4)

$$t' = \langle \varphi_A(\mathbf{r} - \mathbf{R}_A) | H | \varphi_A(\mathbf{r} - (\mathbf{R}_A \pm \mathbf{a})) \rangle$$
 (5)

and

$$t = \langle \varphi_A(\mathbf{r} - \mathbf{R}_A) | H | \varphi_B(\mathbf{r} - (\mathbf{R}_A + a/\sqrt{3}y)) \rangle$$

= $\langle \varphi_A(\mathbf{r} - \mathbf{R}_A) | H | \varphi_B(\mathbf{r} - (\mathbf{R}_A \pm a/2\mathbf{x} + a/(2\sqrt{3})\mathbf{y})) \rangle$, (6)

where H is the Hamiltonian of the solid, and ϕ_A (ϕ_B) denote the $2p_z$ atomic wave function centered on the A (B) atom. Hence, taking $\varepsilon_{2p} = 0$, the solution to equation (1) is

$$E^{\alpha}(\mathbf{k}) = 2t' \cos\left(k_x a\right)$$

$$+ \alpha t \sqrt{1 + 4\cos\left(\frac{\sqrt{3}k_y a}{2}\right)\cos\left(\frac{k_x a}{2}\right) + 4\cos^2\left(\frac{k_x a}{2}\right)},$$
(7)

Table 1. Structures, band gaps and overlaps, and electronic energy transfer, t', calculated with t=-2.5 eV of zigzag SWCNTs with ultra-small diameters. All band gaps are direct at the Γ point ($k_y=0$). For the metallic case, all the band overlaps have a maximum at the Γ point and are given as negative gaps.

Band gap obtained by LDA-DFT	t'	Band gap obtained by ANNNTB
+ GW	(ev)	ANNINIB
corrections		(eV)
(eV)		. ,
	-1.323	-1.467
	-1.290	-0.160
-1.0^{a}	-1.233	-1.004
-0.8^{a}	-1.100	-0.800
0.6^{a}	-0.865	0.599
1.1^{b}	-0.370	1.099
	obtained by LDA-DFT + GW corrections (eV) $-1.0^{a} -0.8^{a} 0.6^{a}$	$\begin{array}{ccc} \text{obtained by} & & & \\ \text{LDA-DFT} & & t' \\ + \text{GW} & (\text{eV}) \\ \text{corrections} & & \\ \text{(eV)} & & & \\ & & -1.323 \\ & & -1.290 \\ -1.0^a & & -1.233 \\ -0.8^a & & -1.100 \\ 0.6^a & & -0.865 \\ \end{array}$

^a From reference [15]. ^b Calculated from references [24,25].

where $\alpha = \pm 1$. In this manner,

$$E_{(n,0)} = E_q^{\alpha}(k_y) = |t| \left[-2\gamma \cos\left(\frac{2q\pi}{n}\right) + \alpha\sqrt{1 + 4\cos\left(\frac{\sqrt{3}k_y a}{2}\right)\cos\left(\frac{q\pi}{n}\right) + 4\cos^2\left(\frac{q\pi}{n}\right)} \right], \quad (8)$$

with

$$\begin{cases} k_x a = \frac{2\pi}{n} q, & (q = 1, 2, \dots, 2n) \\ k_y a = \frac{2\pi}{\sqrt{3}L} m, & (m = -\frac{L}{2}, -\frac{L}{2} + 1, \dots, \frac{L}{2} - 1). \end{cases}$$
(9)

We use t=-2.5 eV, $t'=\gamma t$ and L=1000. We note that values a little below or above L=1000 yield results very near to those calculated with this value and thus our results shall be near to those of a nanotube with infinite length.

The value of t' depends on the diameter of the SWCNT. It was obtained by making the value of the band gap (overlap), which is obtained from the electronic band structure calculated from equation (8), equal to that calculated ab initio. As LDA tends to underestimate the band gap of semiconductors [13,20], Miyake and Saito included many-body effects between electrons using GW approximation (GWA) [20]. They calculated the band gap of the (7,0) SWCNT and the band overlaps of the (5,0) and (6,0) SWCNTs (see Tab. 1).

Sparatu et al. calculated the band gap of the (8, 0) SWCNT using the GW corrections to LDA and found a value of 1.75 eV, which is much larger than the value of 0.60 eV found only with LDA [27,28]. Nevertheless, the lowest optical transition energy obtained with GWA is not in agreement with experimental data, but when the electron-hole (e-h) interaction is included, the lowest optical transition energy of the (8, 0) SWCNT becomes 1.55 eV and agrees well with the available experimental data [27,28]. Hence, the value of the band gap decreases

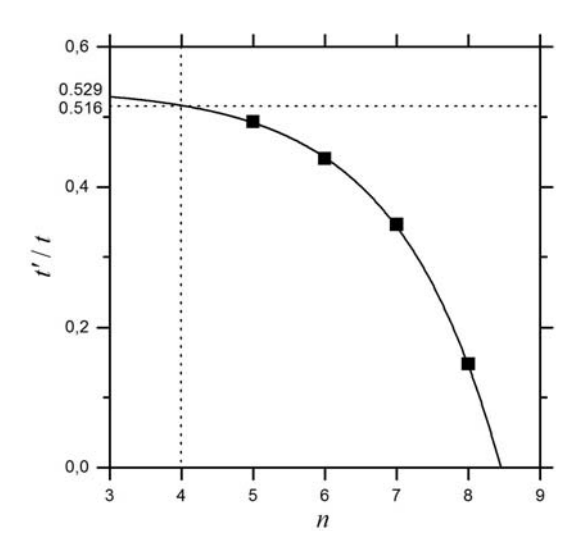


Fig. 2. Electron transfer energy of the anisotropic hopping between next-nearest-neighbor π orbitals (t') relative to t versus the n chiral index. The black squares are points obtained from ab nitio fitting results. The full line is obtained by the function $t'/t = 0.54095 - 0.00154/(1 + 0.00025n)^{-1/0.00036}$. With this function we found the value of t'/t for n=3 and 4.

to a maximum value of 1.55 eV. Assuming that the band gap calculated with the e-h interaction decreases relative to the band gap calculated with GWA only at the same proportion as the lowest optical transition energy, then the band gap of the (8, 0) SWCNT becomes 1.1 eV.

Sparatu et al. showed that the e-h interaction only slightly alters the lowest optical transition energy of the (5, 0) SWCNT relative to the energy calculated with GWA only and that both energies are in very good quantitative agreement with experiments [27,28]. Thus, we expected that the band overlaps of the (5, 0) SWCNT calculated with the GW approximation and including the e-h interaction are close to one another. As the e-h interactions are mainly important for semiconducting SWCNTs [27,28], we expected the band overlap of the (6, 0) SWCNT to be near the overlap calculated by Miyake and Saito using GWA only [20]. The (7, 0) SWCNT is a semiconductor, although the lowest optical transition energy calculated with GWA only (1.2 eV) is very close to the value of 1.289 eV predicted by empirical formulas [29]. Thus, we expected the band gap of the (7, 0) SWCNT calculated with GWA only to be close to the real value as well.

Therefore, the band gaps (overlaps) used to obtain the t' parameters of the (5, 0), (6, 0), and (7, 0) SWCNTs are those calculated with the GW approximation reported in reference [20], while the t' parameter of the (8, 0) SWCNT was calculated from the results reported in references [27,28]. All of the band gaps and overlaps calculated by ANNNTB are equal to those calculated using LDA-DFT including many-body effects between electrons, as can be seen in Table 1.

Figure 2 shows the dependence of t'/t on the chiral index n of the zigzag SWCNT. The amplitude of t' decreases with increasing n and, from a hyperbolic fit of γ (full line in Fig. 2), it cancels the anisotropy (t' = 0) to the zigzag

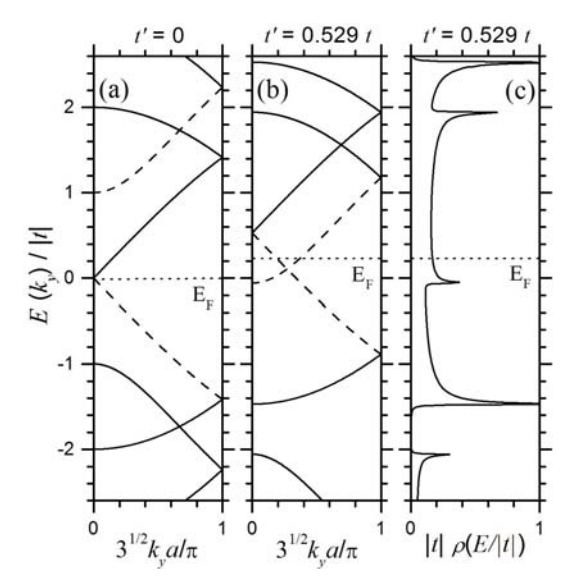


Fig. 3. (3, 0) zigzag SWCNT. Electronic band structure calculated by (a) NNTB and (b) ANNNTB, and (c) density of states calculated by ANNNTB. The dotted line denotes the Fermi level $E_{\rm F}$. The dashed line above the Fermi level is the conduction band, q=n, while the dashed line below the Fermi level is the energy band which become the higher occupied valence band when the ANNNTB model is used.

SWCNTs with n>8. This decrease in t' with increasing diameters of the zigzag SWCNT $(d=na/\pi)$ is physically consistent, i.e., when the diameter of the SWCNT decreases, its curvature becomes larger, causing the distance between the π orbitals located at the same plane perpendicular to the longitudinal axis of the SWCNT (see Fig. 1) to be smaller than that in a SWCNT of greater diameter, and hence the hopping t' increases. The hyperbolic fitting of the ab initio results gives us possible values for the γ parameter for the (3,0) and (4,0) SWCNTs (Fig. 2). These parameters were utilized to obtain the band overlaps of the (3,0) and (4,0) SWCNTs by means of the band structures calculated by equation (8) (see Tab. 1).

3 Results and discussions

The NNTB (t'=0) and ANNNTB band structures of (n,0) zigzag SWCNTs with n=3,4,5,6,7, and 8 are shown in Figures 3–8, respectively, together with the densities of states (ρ) . The (4,0) and (5,0) SWCNTs, which are predicted by the 1/3 rule to be semiconductors (see Figs. 4a and 5a), present band overlaps (see Figs. 4b and 5b) when the ANNNTB model is used. We found by ANNNTB that the band gap of the (4,0) SWCNT obtained by NNTB vanishes for $\gamma \geq 0.500$. The metallicity of the (4,0) and (5,0) SWCNTs has been reported in various previous works based on ab initio calculations [14-24,28], but it is believed that a π orbital-only tight-binding model is not able to obtain these properties.

The band structures of the (3, 0) and (6, 0) SWCNTs also present band overlaps that are not predicted by the NNTB model (see Figs. 3a and 3b, and Figs. 6a and 6b).

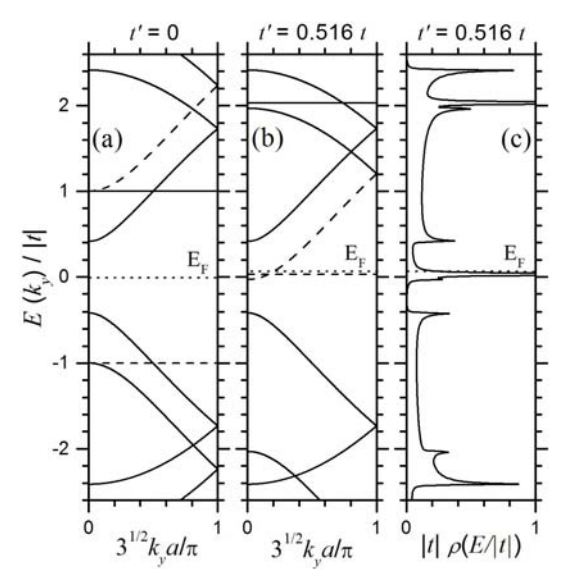


Fig. 4. (4, 0) zigzag SWCNT. Electronic band structure calculated by (a) NNTB and (b) ANNNTB, and (c) density of states calculated by ANNNTB. The dotted line denotes the Fermi level $E_{\rm F}$. The dashed line above the Fermi level is the conduction band, q=n, while the dashed line below the Fermi level is the energy band which become the higher occupied valence band when the ANNNTB model is used.

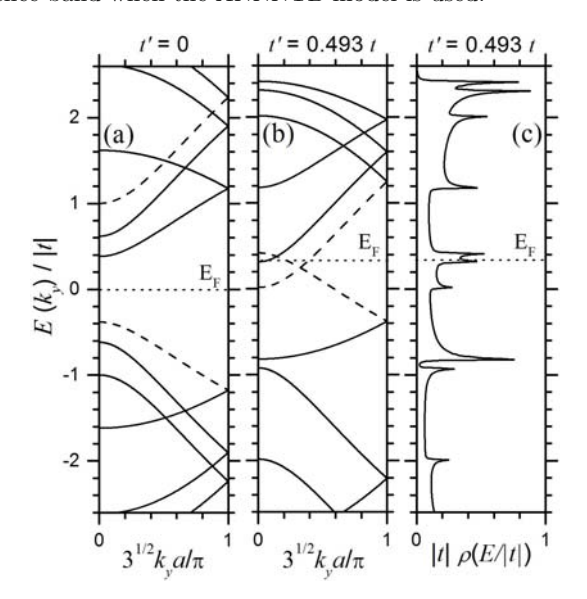


Fig. 5. (5, 0) zigzag SWCNT. Electronic band structure calculated by (a) NNTB and (b) ANNNTB, and (c) density of states calculated by ANNNTB. The dotted line denotes the Fermi level $E_{\rm F}$. The dashed line above the Fermi level is the conduction band, q=n, while the dashed line below the Fermi level is the energy band which become the higher occupied valence band when the ANNNTB model is used.

The existence of band overlapping in the band structure of the (6,0) SWNCT obtained by ANNNTB agrees with the LDA-DFT calculations with [20] and without [13] GW corrections, but we did not find electronic band structure calculations for the (3,0) SWCNT in the literature to make comparisons. Barone and Scuseria confirmed by means of a systematic DFT study that the (3,0) SWCNT

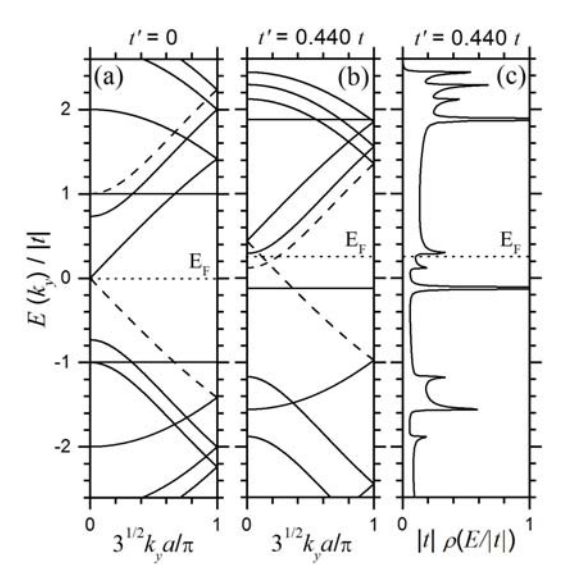


Fig. 6. (6, 0) zigzag SWCNT. Electronic band structure calculated by (a) NNTB and (b) ANNNTB, and (c) density of states calculated by ANNNTB. The dotted line denotes the Fermi level $E_{\rm F}$. The dashed line above the Fermi level is the conduction band, q=n, while the dashed line below the Fermi level is the energy band which become the higher occupied valence band when the ANNNTB model is used.

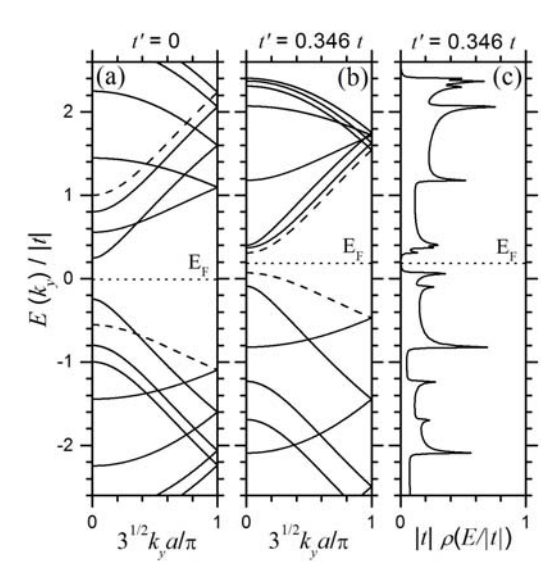


Fig. 7. (7, 0) zigzag SWCNT. Electronic band structure calculated by (a) NNTB and (b) ANNNTB, and (c) density of states calculated by ANNNTB. The dotted line denotes the Fermi level $E_{\rm F}$. The dashed line above the Fermi level is the conduction band, q=n, while the dashed line below the Fermi level is the energy band which become the higher occupied valence band when the ANNNTB model is used.

is a metal [23], but they did not present the band structure and did not report the value of a possible band overlap.

The band structures determined by NNTB and ANNNTB showed that both the (7, 0) SWCNT (see Figs. 7a and 7b) and the (8, 0) SWCNT (see Figs. 8a and 8b) are semiconductors, although the band gaps calculated with ANNNTB are smaller than those calculated

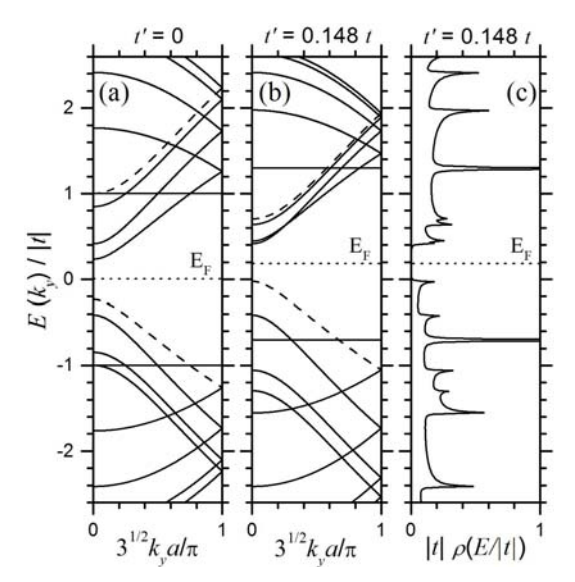


Fig. 8. (8, 0) zigzag SWCNT. Electronic band structure calculated by (a) NNTB and (b) ANNNTB, and (c) density of states calculated by ANNNTB. The dotted line denotes the Fermi level $E_{\rm F}$. The dashed line above the Fermi level is the conduction band, q=n, while the dashed line below the Fermi level is the energy band which become the higher occupied valence band when the ANNNTB model is used.

with NNTB. Thus, the band gaps of the (7,0) and (8,0) SWCNT calculated with ANNNTB are in agreement with the 1/3 rule, but break the 1/d rule because the band gap of the (8,0) SWCNT is larger than that of the band gap of the (7,0) SWCNT. These results agree with the various results obtained by ab initio calculations [13–15].

The metallic or semiconductor characteristics of the SWCNTs obtained by band structures using the ANNNTB model can be found from the densities of states shown in Figures 3c–8c. The densities of states were calculated by the expression:

$$\rho(E) = -\operatorname{Im} \frac{1}{\pi N_C} \sum_{k_y} \sum_{\alpha, q} \frac{1}{E - E_q^{\alpha}(k_y) + i\delta}; \qquad (10)$$

where N_C denotes the number of carbon atoms of the SWCNT, and δ is an appropriate broadening factor, as usual [26]. Our tests revealed that 0.005|t| is an adequate value for δ . The Fermi level of the semiconductor SWCNTs was placed in the middle of the band gap.

We found a large van Hove peak for the (4, 0) SWCNT just below the Fermi level (see Fig. 4c), which is in excellent agreement with ab initio results [21,24]. The densities of states of the (3, 0), (4, 0), and (5, 0) SWCNTs (see Figs. 3c–5c, respectively) present a gap in the valence band that was not found by either NNTB (indicated by band structures shown in Figures 4a–6a) or DFT calculations [17,19,21,24,28]. This result clearly reveals that the hopping anisotropic between next-nearest-neighbor sites increases the distance between the valence bands. The densities of states at the Fermi level of the (5, 0) and (6, 0) SWCNTs calculated with the LDA-DFT are equal to 0.35 states/eV per atom [17] and 0.07 states/eV per

atom [13], respectively, while we obtained 0.20 states/eV per atom and 0.04 states/eV per atom, respectively, by ANNNTB calculations.

The band structures calculated with the ANNNTB model reveal that the maximum band overlaps of the metallic (3,0), (4,0), (5,0), and (6,0) SWCNTs occur at the Γ point and the band gaps of the semiconductor (7,0) and (8,0) SWCNTs are direct and also at the Γ point (see Figs. 3b–8b). These results agree with both LDA [13,16–20] and GWA [20,27,28] calculations applied to the (5,0), (6,0), (7,0), and (8,0) SWCNTs.

The band overlaps of the zigzag SWCNTs with n=3, 4, 5, and 6 predicted by the ANNNTB model occur because the non-degenerate conduction band with quantum number q=n is lower in energy and a doubly degenerate valence band is higher in energy (dashed lines in Figs. 3b–6b) relative to their respective positions in the band structures calculated by NNTB (dashed lines in Figs. 3a–6a).

The reason why the q=n conduction band is lower in energy is because the term of the anisotropy in equation (8) (term multiplied by γ) has the minimum value at this point, and this occurs because in the lattice utilized to generate the zigzag SWCNTs studied here (see Fig. 1b), the distance along the direction of the chiral vector between next-nearest-neighbor sites is twice the distance between nearest-neighbor sites.

This downshift of the non-degenerate conduction band was first found by Blase et al. while studying the (6, 0)SWCNT via LDA-DFT calculations [13], and it was interpreted as being due to a strong $\pi^* - \sigma^*$ hybridization. However, they did not explain why the conduction band, which causes the band overlap of the (6, 0) SWCNT, is non-degenerate. Blase et al. also reported that the same non-degenerate band is responsible for the reduction of the band gaps of the (7, 0) and (8, 0) SWCNTs below those calculated by the NNTB model [13]. However, we found by ANNNTB calculations, that the q = n non-degenerate conduction band is only responsible for the reduction of the band gap of the (7, 0) SWCNT (see Figs. 7b and 8b). The band gap of the (8, 0) SWCNT calculated by the ANNNTB model is smaller than that obtained by the NNTB model due to the approximation of two doubly degenerate bands.

Reich et al. showed that the NNTB model provides an adequate description of the valence band of the (10, 0) SWCNT when compared with that obtained by LDA [25], although the NNTB model is not able to reproduce band structure above the Fermi level. They verify that the differences in energy between the conduction bands at the Γ point, which is the critical point from which the singularities in the density of states originate, are vastly exaggerated by NNTB. However, our results for zigzag SWCNTs with n = 3, 4, 5, 6, 7, and 8 obtained by ANNNTB also present differences in energy between the conduction bands at the Γ point smaller than that obtained by NNTB, but the differences in energy between the valence bands at the same point are higher than that obtained by NNTB as can be verified by comparing Figures 3a-8a with Figures 3b–8b, respectively.

4 Conclusions

(n, 0) single-wall carbon nanotubes studied (SWCNTs) with chiral index n ranging from 3 to 8, that is, zigzag SWCNTs with diameters smaller than 0.7 nm. The ultra-small diameters of these nanotubes cause the breakage of the 1/3 and 1/d rules. The standard explanation attributes this phenomenon to the strong hybridization of the π^* and σ^* states induced by the large curvature of these SWCNTs. In this work we proposed a π orbital-only tight-binding model including anisotropy in the hopping between next-nearest-neighbor sites (ANNNTB). We showed that it is able to describe both the band overlaps and gaps of zigzag ultra-small SWCNTs obtained by ab initio calculations. The anisotropy causes the approximation of the conduction bands and the separation of the valence bands relative to the band structures calculated by nearest-neighbor tight-binding (NNTB). And thus this causes the band overlaps in the electronic band structures of zigzag SWCNTs with n = 3, 4, 5, and 6, indicating that they are metals, and also causes the decrease of the band gaps of the semiconductors (7, 0) and (8, 0) SWCNTs relative to those obtained from the NNTB model. The ANNNTB model yielded a natural explanation to the fact that armchair and chiral SWCNTs are less affected by curvature than zigzag SWCNTs as well as yielded a reason why non-degenerate states cause band overlaps of zigzag SWCNTs with n = 3, 4, 5, and 6.

We would like to express our sincere thanks to M.E. de Souza for valuable comments. This work was supported by the CAPES and CNPq (Brazilian agencies).

References

- 1. S. Iijima, Nature (London) **354**, 56 (1991)
- 2. P.M. Ajayan, S. Iijima, Nature (London) **358**, 23 (1992)
- L.F. Sun, S.S. Xie, W. Liu, W.Y. Zhou, Z.Q. Liu, D.S. Tang, G. Wang, L.X. Qian, Nature (London) 403, 384 (2000)
- 4. L. Qin, X. Zhao, K. Hirahara, Y. Miyamoto, Y. Ando, S. Iijima, Nature (London) 408, 50 (2000)

- N. Wang, Z.K. Tang, G.D. Li, J.S. Chen, Nature (London) 408, 50 (2000)
- L.-M. Peng, Z.L. Zhang, Z.Q. Xue, Q.D. Wu, Z.N. Gu, D.G. Pettifor, Phys. Rev. Lett. 85, 3249 (2000)
- X. Zhao, Y. Liu, S. Inoue, T. Suzuki, R.O. Jones, Y. Ando, Phys. Rev. Lett. 92, 125502 (2004)
- 8. L. Guan, K. Suenaga, S. Iijima, Nano Lett. 8, 459 (2008)
- R. Saito, G. Dresselhaus, M.S. Dresselhaus, Physical Properties of Carbon Nanotubes, 1st edn. (Imperial College, London, 1998)
- R. Saito, M. Fujita, G. Dresselhaus, M.S. Dresselhaus, Appl. Phys. Lett. 60, 2204 (1992)
- N. Hamada, S. Sawada, A. Oshiyama, Phys. Rev Lett. 68, 1579 (1992)
- C.T. White, D.H. Robertson, J.W. Mintmire, Phys. Rev. B 47, 5485 (1993)
- X. Blase, L.X. Benedict, E.L. Shirley, S.G. Louie, Phys. Rev. Lett. **72**, 1878 (1994)
- O. Gülseren, T. Yildirim, S. Ciraci, Phys. Rev. B 65, 153405 (2002)
- 15. V. Zólyomi, J. Kürti, Phys. Rev. B 70, 085403 (2004)
- Z.M. Li, Z.K. Tang, H.J. Liu, N. Wang, C.T. Chan, R. Saito, S. Okada, G.D. Li, J.S. Chen, N. Nagasawa, S. Tsuda, Phys. Rev. Lett. 87, 127401 (2001)
- 17. H.J. Liu, C.T. Chan, Phys. Rev. B 66, 115416 (2002)
- 18. M. Machón, S. Reich, C. Thomsen, D. Sánchez-Portal, P. Ordejón, Phys. Rev. B **66**, 155410 (2002)
- I. Cabria, J.W. Mintmire, C.T. White, Phys. Rev. B 67, 121406 (2003)
- 20. T. Miyake, S. Saito, Phys. Rev. B 68, 155424 (2003)
- J.T. Titantah, K. Jorissen, D. Lamoen, Phys. Rev. B 69, 125406 (2004)
- Y.L. Mao, X.H. Yan, Y. Xiao, J. Xiang, Y.R. Yang, H.L. Yu, Nanotechnology 15, 1000 (2004)
- 23. V. Barone, G. Scuseria, J. Chem. Phys. 121, 10376 (2004)
- 24. M.R. Mohammadizadeh, Physica E 31, 31 (2006)
- S. Reich, C. Thomsen, P. Ordejón, Phys. Rev. B 65, 155411 (2002)
- 26. H. Yorikawa, S. Muramatsu, Phys. Rev. B 52, 2723 (1995)
- C.D. Sparatu, S. Ismail-Beigi, L.X. Benedict, S.G. Louie, Phys. Rev. Lett. 92, 077402 (2004)
- 28. C.D. Sparatu, S. Ismail-Beigi, L.X. Benedict, S.G. Louie, Appl. Phys. A 78, 1129 (2004)
- 29. R.B. Weisman, S.M. Bachilo, Nano Lett. 3, 1235 (2003)